

PCCP

Accepted Manuscript



This is an *Accepted Manuscript*, which has been through the Royal Society of Chemistry peer review process and has been accepted for publication.

Accepted Manuscripts are published online shortly after acceptance, before technical editing, formatting and proof reading. Using this free service, authors can make their results available to the community, in citable form, before we publish the edited article. We will replace this *Accepted Manuscript* with the edited and formatted *Advance Article* as soon as it is available.

You can find more information about *Accepted Manuscripts* in the [Information for Authors](#).

Please note that technical editing may introduce minor changes to the text and/or graphics, which may alter content. The journal's standard [Terms & Conditions](#) and the [Ethical guidelines](#) still apply. In no event shall the Royal Society of Chemistry be held responsible for any errors or omissions in this *Accepted Manuscript* or any consequences arising from the use of any information it contains.

ARTICLE

Theoretical survey of the ligand tunability of poly(azolyl)borates

Cite this: DOI: 10.1039/x0xx00000x

Dongmei Lu^a and Huarong Tang^bReceived 00th January 2012,
Accepted 00th January 2012

DOI: 10.1039/x0xx00000x

www.rsc.org/

Using density functional calculations, we have systematically investigated a series of homoleptic poly(azolyl)borate ligands, which display unusual steadily declining bond strengths accompanied by bond contractions when the azolyl groups are sequentially substituted to the parent BH_4^- . As ligands, their effects on the coordinated metal ions (Cu(I) and Mo(0)) are quantitatively represented by two ligand tunability descriptors: the vibration frequency (ν_{CO}) of the CO groups complexed to the metal ions and the charge of the metal-(CO)_x moiety, between which a good linear correlation exists. For the same number of azolyl substitutions, the boundary of ligand tunability is always marked by the pyrazolyl and tetrazolyl groups at the two ends, which feature the lowest and the highest nitrogen content in the azolyl ring, respectively. With the increase of azolyl substitution number in the borate ligands, the ν_{CO} range expands, indicating a higher tunability of the ligands. The type of metal ion and the charge it carries play minor roles in influencing the ligand tunability.

Introduction

Since the first synthesis of the famous scorpionate ligands of hydrotris(pyrazolyl)borates by Trofimenko in 1966,^{1,2} various poly(azolyl)borates have been developed over nearly the past five decades.³⁻¹⁸ With the recent synthetic advances^{19,20}, a full family picture of these ligands centered with a tetrahedral boron bearing all kinds of five-membered N-heterocyclic (NHC) groups is becoming complete (Figure 1).²¹⁻²³ As key components in mimics of metalloproteins, they have shown potentials in bioinorganic and medicinal chemistry, going far beyond the traditional inorganic chemistry.²⁴⁻²⁷ In various metal complexes, these borate ligands determine the key properties, such like the solubility and the cell passing ability through changing the balance between hydrophilicity and lipophilicity, the stability toward trans-chelation reactions and metal-disproportionation reactions, which are crucial for the metal center to properly function.

More importantly, as spectator ligands in biomimetics, their influence on the electronic structure of the coordinated metal is the center of concern, which can be well characterized by the shift of the vibration frequency of the bound carbonyl groups.²⁸ Particularly, Casarin et. al. have not only computationally reproduced the experimentally observed red shifts of the CO vibrations (compared to free CO) in the [Cu(borate)(CO)] complexes consisting of pyrazolyl and 1,2,4-triazolyl groups, but also through comprehensive electronic structure analyses, they have shown that the two ligands are electronically equivalent to each other, with the 1,2,4-triazolyl group providing better bio-compatible properties.²⁹⁻³¹ In addition, the Elliott group has theoretically studied CO vibrations in a series of [Mo(0)(borate)(CO)₃]⁻ complexes, with the tripodal borate ligands composed of mixed azolyl groups (including pyrazolyl

and 1,2,4-triazolyl groups) and structurally close-related carbenes.³² The carbene-azolyl mixed borate ligands are found to be able to tune the electronic structure of the metal substantially. However, a full-scale survey of the tunability of the poly(azolyl)borates ligand family is still lacking.

In this study, we utilize calculations based on density functional theory (DFT) to answer the question. We consider the structurally representative homoleptic poly(azolyl)borate ligands. The azolyl groups include five-membered NHC rings with one to four nitrogen atoms and some of their benzazole counterparts that can form scorpionates. We first investigate the interactions between the boron center and the (benz)azolyl rings, with a focus on the sequential (step-wise) bond formation energy and geometry changes along with the increasing number of the rings and the natural bond orbital (NBO) charge on boron. Then, we construct a [M(L)_n(CO)_x] model to evaluate the ligand tunability in terms of metal ions (M = Cu(I), Mo(0)), number of (benz)azolyl rings ($n = 2$ to 4), and the corresponding complexed number of CO moieties (for Cu, $x = 1, 2$; for Mo, $x = 3, 4$). We select Cu(I), one of the most often encountered metal species in biological processes, and Mo(0), the only second row transition metal essential to life, as the representative metal ions.²⁴ By calculating the vibration frequency of the attached CO (ν_{CO}), we map out the range of the ligand tunability. Finally, we correlate ν_{CO} with the NBO charge on the M(CO)_x moiety, which is directly influenced by the borate ligands through their electronic and steric effects.

Calculation methods

All calculations were performed with the Gaussian 09 suite of programs.³³ We followed the widely used DFT protocol (B3LYP/6-31++G(p,d))^{34,35} for optimization and frequency calculations. For Cu and Mo, the SDD basis set were employed instead.^{36,37} The zero

point energy corrected 0K energies were used for calculating the sequential bond formation energies between the boron center and the azolyl group, which is defined according to the following simple hypothetical reaction (see details in B subsection, Results):



$$E_b = E[\text{BH}_{(4-(n+1))}(\text{azolyl})_{(n+1)}] + E(\text{H}_2) -$$

$$E[\text{BH}_{(4-n)}(\text{azolyl})_n] - E[\text{azole}] \quad (2).$$

E_b is the bond formation energy indicating the B-N bond strength. Other E 's are the 0 K energy of the corresponding species. NBO charges were calculated using the NBO 3 program implemented in the Gaussian 09 suite.³⁸

Results and discussion

A. Homoleptic poly(azolyl)borate ligands

Thanks to the long term efforts of synthetic chemists, the homoleptic poly(azolyl)borate ligand family consisting of five-membered NHC rings and their benzene annelated derivatives can now be sketched out in nearly completion (Figure 1). In each row, the number of azolyl rings increases from one to four. Descending the rows, the number of N atoms in a ring increases from one to four, exhausting all possible configurations. For benzazoles, only indazole and benzotriazole are selected, as their borates can multidentately coordinate to the same metal ion as pincer ligands. Multiple positions of N connecting to the boron atom are possible for triazolyl and tetrazolyl rings and the interconversion of the regioisomers is possible.^{20, 39} By selecting metal ions, these ligands can form either coordination polymers or homoleptic complexes. For the sake of conciseness, *only* the configurations of homoleptic complexes linking at N1 are considered here.

The missing ones (in red) are either due to difficulty in synthesis of installing more azolyl rings to the boron center or due to their little interests as useful pincer ligands bearing only a single azolyl ring. Though most of the mono(azolyl)borate ligands are not even explicitly reported in experiment, their azolyl-boron bond formation energies will make the analysis of the sequential binding trend complete. For the bis(azolyl)borates, their coordination with metal ions are different than the tris and tetrakis ones and will be discussed separately. Tris(azolyl)borates are always the focus of the scorpionate ligand family and their syntheses have been completed by the final addition of tris(1,2,3-triazolyl) borates in the last year.²⁰ Tris- and tetrakis(azolyl)borate ligands are expected to present similar tunability, as the fourth azolyl group is pretty much only a spectator in the face capping κ^3 -ligand-metal complex.

B. Sequentially changing properties

Using DFT, we obtain the structural information of the ligands shown in Figure 1. We focus on the sequential changes in geometry and the B-N and B-H bond strengths as a function of the increasing number of azolyl rings (Table 1). We notice that for all types of azolyl rings regardless of the N content, the NBO charge on the boron atom changes from $-0.7 e$ when no ring installed (BH_4^-) to $+1.0 e$ when four rings attached with a rate of $\sim 0.4 e$ charge transfer away from the boron center per

additional ring. Moreover, the sequential bond formation energy rises quickly (less exothermic) along with the increasing number of azolyl rings. In general, the fourth B-N bond strength reduces by half compared with that of the first. The synthesis of borates with higher number of azolyl substitutions must become harder.

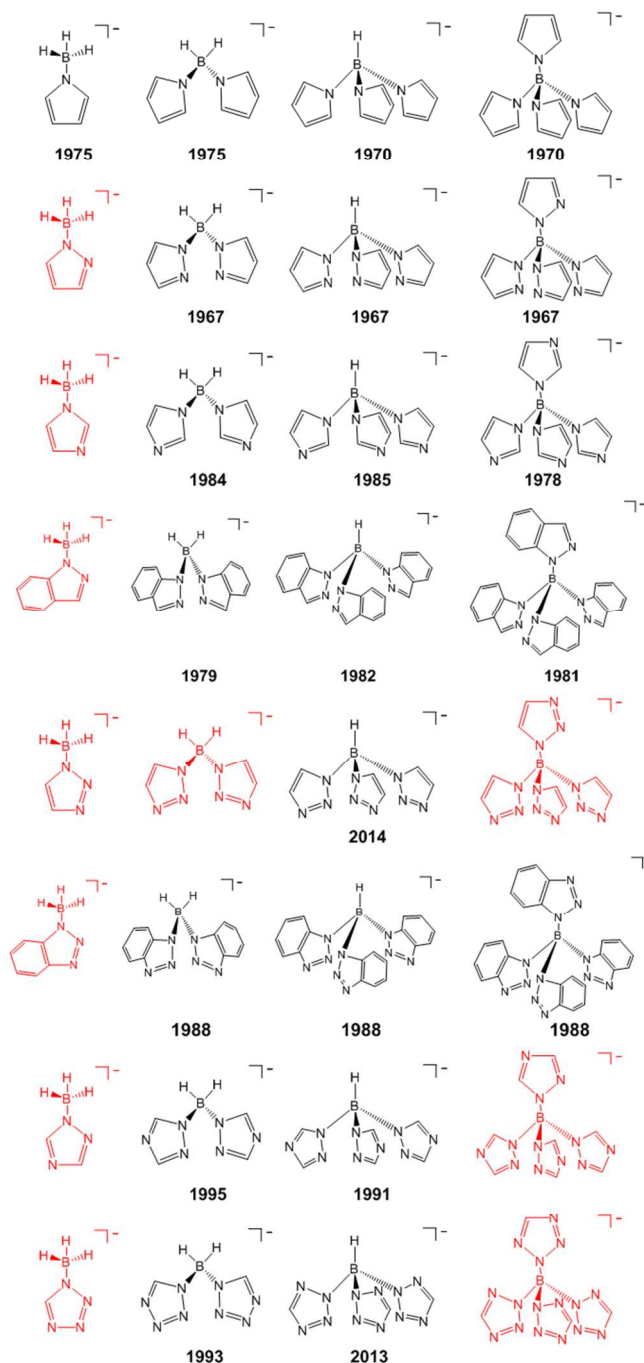


Figure 1. Homoleptic poly(azolyl)borate ligands studied in this work. Five-membered NHC azolyl groups and some benzazolyl groups are included. The first synthesis date of each ligand is labelled below the corresponding structure. The red structures have not been reported yet.

Table 1. Calculated sequentially changing properties of poly(azolyl)borate ligands.¹

ligand	d_{B-N}^2	d_{B-H}^3	$e(B)^4$	E_b^5
$[BH_4]^-$	--	1.240	-0.686	--
$[BH_3(\text{pyrr}^{[6]})]^-$	1.582	1.229	-0.165	-96.9
$[BH_2(\text{pyrr})_2]^-$	1.568	1.216	0.267	-89.9
$[BH(\text{pyrr})_3]^-$	1.558	1.212	0.676	-75.9
$[B(\text{pyrr})_4]^-$	1.559	--	1.123	-54.0
$[BH_3(\text{pyra})]^-$	1.582	1.225	-0.162	-105.7
$[BH_2(\text{pyra})_2]^-$	1.567	1.209	0.251	-98.6
$[BH(\text{pyra})_3]^-$	1.561	1.196	0.660	-74.9
$[B(\text{pyra})_4]^-$	1.540- 1.570	--	1.091	-50.9
$[BH_3(\text{imi})]^-$	1.584	1.226	-0.169	-125.9
$[BH_2(\text{imi})_2]^-$	1.568	1.213	0.251	-108.9
$[BH(\text{imi})_3]^-$	1.557	1.208	0.657	-88.0
$[B(\text{imi})_4]^-$	1.554- 1.556	--	1.094	-63.4
$[BH_3(\text{inda})]^-$	1.583	1.227	-0.177	-123.6
$[BH_2(\text{inda})_2]^-$	1.562	1.213	0.244	-101.4
$[BH(\text{inda})_3]^-$	1.549	1.212	0.640	-78.3
$[B(\text{inda})_4]^-$	1.554- 1.568	--	1.092	-41.5
$[BH_3(\text{tria124})]^-$	1.583	1.224	-0.167	-139.2
$[BH_2(\text{tria124})_2]^-$	1.564	1.208	0.241	-121.4
$[BH(\text{tria124})_3]^-$	1.552	1.119	0.637	-92.7
$[B(\text{tria124})_4]^-$	1.548	--	1.057	-75.0
$[BH_3(\text{tria123})]^-$	1.588	1.223	-0.170	-142.1
$[BH_2(\text{tria123})_2]^-$	1.571	1.205	0.232	-124.6
$[BH(\text{tria123})_3]^-$	1.556	1.194	0.628	-93.3
$[B(\text{tria123})_4]^-$	1.551	--	1.060	-71.8
$[BH_3(\text{bentria})]^-$	1.585	1.224	-0.189	-152.7
$[BH_2(\text{bentria})_2]^-$	1.573	1.211	0.231	-114.7
$[BH(\text{bentria})_3]^-$	1.548	1.21	0.625	-82.6
$[B(\text{bentria})_4]^-$	1.549- 1.566	--	1.063	-53.2
$[BH_3(\text{tetr})]^-$	1.589	1.222	-0.175	-181.6
$[BH_2(\text{tetr})_2]^-$	1.568	1.204	0.223	-147.7
$[BH(\text{tetr})_3]^-$	1.552	1.194	0.616	-106.7
$[B(\text{tetr})_4]^-$	1.546	--	1.032	-81.2

Notes: [1] The sequentially changing properties include the key geometric parameters (B-H and B-N bond lengths), the NBO charges on boron, and the B-N bond formation energies after each installation of azolyl groups to the boron center. [2] The bond (Å) between the linking N atom of the azolyl group and the boron atom. In bis-, tris-, and some tetrakis(azolyl)borates, only one B-N bond length is reported, as the B-N bonds are identical. In other tetradentate ligands, four B-N bonds are different, and the shortest and the longest bonds are reported. [3] The bond (Å) between the boron atom and the H atoms. Only one B-H bond length is reported, as the B-H bonds are identical. [4] NBO charge on the boron atom. [5] Sequential bond formation energy (E_b , kJ/mol) is defined in eq (1) and (2). [6] Abbreviations used: pyrr = pyrrolyl; pyra = pyrazolyl; imi = imidazolyl; inda = indazolyl; tria124 = 1,2,4-triazolyl; tria123 = 1,2,3-triazolyl; bentria = benzotriazolyl; tetr = tetrazolyl.

Furthermore, the sequential B-N bond formation energy linearly correlates with the corresponding NBO boron charge (Figure 2), which reflects the fact that the similar amount of charge transfer from the boron to the rings accompanying the increasing number of rings becomes less effective in stabilizing

the structure. The reason is that the rings compete for the same resource (electron, space, etc.) and effectively repel each other, analogous to the commonly known "coverage effects" in heterogeneous catalysis.^{40, 41} The tetrazolyl-boron bond is always the strongest among all the B-N bonds throughout one to four ring installations, as the four more electronegative N atoms in the ring can better accommodate the negative charge transferred from the boron center to the ring(s).

Notably, when the number of rings increases from one to three, both the B-N and B-H bonds become shorter, also suggesting the azolyl rings can hold the negative charge better than the tetrahedral boron. The poly(azolyl)borate ligands serve as an additional case of the breakdown of generally believed "bond length-bond strength correlation".⁴²⁻⁴⁵ As the negative charge transfers away from the boron to more electronegative groups, the boron's effective size shrinks, which leads to a larger disparity in its *s* and *p* orbitals, eventually causing the so-called "hybridization defects"⁴⁶ and consequently the less efficient covalent bonding between B and N or H. The shrinkage of the boron size dominates the change, thus shorter but weaker B-N and B-H bonds are formed.⁴²

From tris to tetrakis substitutions, the B-N bond length change is complicated by the ensuing lower degree of ligand symmetry: some of the bonds further shorten while the others slightly stretch. For single ring substitution of BH_4^- , the five-membered azolyl rings feature weaker binding compared to their benzene annelated derivatives. As more substitutions take place, the trends of the bond strength overlap and no clear pattern is observed.

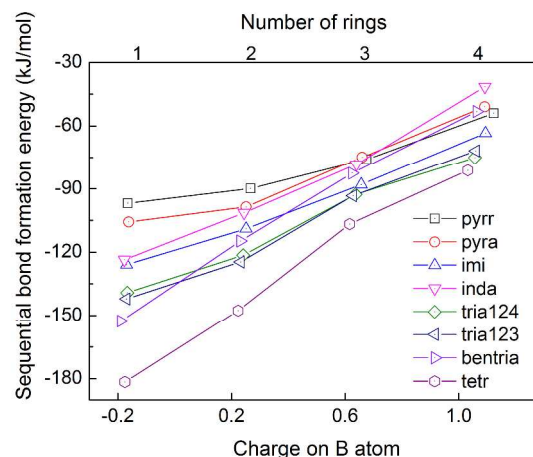


Figure 2. The sequential bond formation energy of poly(azolyl)borate ligands versus the NBO charge on boron. For the full names of the azolyl groups, see Table 1.

C. Model to evaluate the ligand tunability

We employ a model of $[M(L)_n(CO)_x]$ ($M = Cu(I), Mo(0)$; $L =$ the number of azolyl groups of the borate ligand; $n = 2$ to 4 ; x depends on M and n) to evaluate the ligand tunability in terms of the attached CO vibration frequency shift. $Cu(I)$ and $Mo(0)$ respectively represent the first and the second row transition metals and both of which are of special importance in bioinorganic chemical processes.^{29, 32} Furthermore, choosing both charged and neutral metal centres, the dependency of ligand tunability on charge can be obtained. In the complexes,

Cu(I) is tetrahedral and Mo(0) is octahedral. For bis(azolyl)borates, there are two and four carbonyl groups bound to the Cu(I) and Mo(0) centers, respectively. For tris- and tetrakis(azolyl)borates, there are one and three carbonyl groups coordinated to the Cu(I) and Mo(0) center, correspondingly.

The model is illustrated in Figure 3 using the poly(pyrazolyl)borate ligands as an example. For the two

groups of $[M(L)_n(CO)_x]$ complexes, the neutral Cu-complexes have shorter N-metal and C-O bonds compared with that of anionic Mo-complexes. For either group of metal complexes, with the fourth pyrazolyl group being the spectator, the tris- and tetrakis(pyrazolyl) borates exhibit very similar geometry in the complexes. While for the bis(pyrazolyl)borates, they only bidentately bind to the metal.

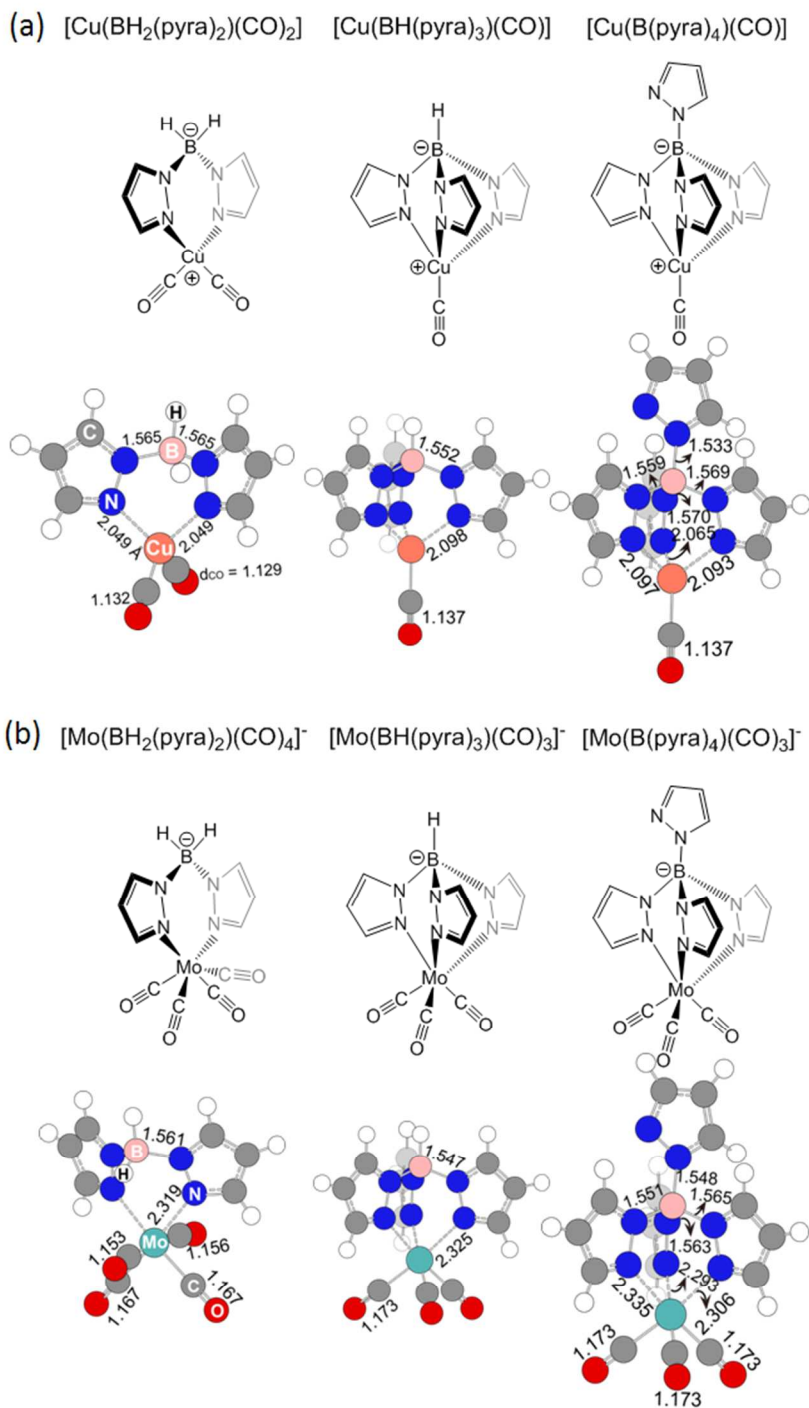


Figure 3. The $[M(L)_n(CO)_x]$ model exemplified by pyrazolyl substitutions. (a) The neutral Cu(I)-complexes. Top and bottom rows are molecular and optimized structures, respectively. The lengths of the metal-N bond, B-N bond, and C-O bond are labelled in the optimized structures. Bonds with identical lengths are labelled once when space is limited. (b) The anionic Mo(0)-complexes.

D. Ligand tunability

Table 2. Calculated geometric parameters, NBO charges, and ν_{CO} of $[\text{Cu}(\text{I})(\text{L})_n(\text{CO})_x]^{-1}$.

ligand	$d_{\text{Cu-N}}^2$	$d_{\text{C-O}}^2$	$e(\text{B})^3$	$e(\text{Cu}(\text{CO})_x)^3$	ν_{CO}
$[\text{BH}_2(\text{pyra})_2]^-$	2.049	1.131	0.232	0.814	2183.3
$[\text{BH}(\text{pyra})_3]^-$	2.098	1.137	0.620	0.799	2145.1
$[\text{B}(\text{pyra})_4]^-$	2.085	1.137	1.082	0.801	2146.1
$[\text{BH}_2(\text{inda})_2]^-$	2.053	1.130	0.227	0.825	2186.2
$[\text{BH}(\text{inda})_3]^-$	2.093	1.137	0.610	0.806	2148.5
$[\text{B}(\text{inda})_4]^-$	2.087	1.137	1.101	0.807	-- ⁴
$[\text{BH}_2(\text{tria124})_2]^-$	2.057	1.129	0.222	0.829	2193.2
$[\text{BH}(\text{tria124})_3]^-$	2.107	1.135	0.602	0.812	2162.8
$[\text{B}(\text{tria124})_4]^-$	2.096	1.135	1.055	0.819	2165.2
$[\text{BH}_2(\text{tria123})_2]^-$	2.059	1.128	0.222	0.835	2197.8
$[\text{BH}(\text{tria123})_3]^-$	2.115	1.133	0.608	0.817	2173.6
$[\text{B}(\text{tria123})_4]^-$	2.104	1.133	1.061	0.824	2177.3
$[\text{BH}_2(\text{bentria})_2]^-$	2.062	1.129	0.216	0.844	2200.6
$[\text{BH}(\text{bentria})_3]^-$	2.111	1.133	0.601	0.824	2175.2
$[\text{B}(\text{bentria})_4]^-$	2.098	1.133	1.078	0.832	-- ⁴
$[\text{BH}_2(\text{tetra})_2]^-$	2.071	1.128	0.215	0.850	2210.5
$[\text{BH}(\text{tetra})_3]^-$	2.130	1.131	0.593	0.834	2194.9
$[\text{B}(\text{tetra})_4]^-$	2.123	1.130	1.036	0.840	2200.2

Notes: [1] $\nu_{\text{CO}}(\text{cm}^{-1})$ is the averaged vibration frequencies of all CO related modes in a complex. $n = 2, x = 2; n = 3 \text{ or } 4, x = 1$. [2] For bonds of the same kind, the average length (\AA) is given here, e.g. for $[\text{CuB}(\text{pyra})_4\text{CO}]$, $d_{\text{Cu-N}}$ is the average of the three Cu-N bonds. [3] NBO charge. [4] The calculation was not complete due to the limited computational resources. For the full names of the azolyl groups, see Table 1.

As we have seen in the above example, the analysis of the geometry is not sufficient for illustrating the tunability of the borate ligands. We now take a look at the charges on the B and $\text{M}(\text{CO})_x$ parts, which may provide more information on the ligand-metal interactions (Table 2 and 3). As the ring substitution increases from two to four, the boron continues to lose electron density, following a quantitatively similar pace as the metal-free borate ligands (Table 1), indicating that the charge mainly transfers to the newly installed azolyl ring and the transfer is affected little by the complexed metal. Meanwhile, the charge on the $\text{M}(\text{CO})_x$ moiety is more or less stable: positive on $\text{Cu}(\text{I})(\text{CO})_x$ and negative on $\text{Mo}(\text{O})(\text{CO})_x$, with a variation less than $0.25 e$, implying the CO vibration frequency change should also be small to moderate in response to different azolyl substitutions.

For the two groups of metal complexes, distinctive differences in all aspects (geometry, charge, CO vibration frequency) must be caused both by the way of metal's coordination and the original charge on the metal. For instance, the longer C-O and metal-N bonds in Mo-complexes compared to that in their Cu counterparts may suggest a different ligand tunability in terms of ν_{CO} in the Cu complexes.

However, essentially, the same range of the ν_{CO} shifts is observed for both groups. For the Cu- and Mo-complexes, the tunability ranges of bis(azolyl)borate ligands are correspondingly ~ 27 and $\sim 24 \text{ cm}^{-1}$, the narrowest of all denticity. The tunability of tris(azolyl)borate ligands are higher ($\sim 50 \text{ cm}^{-1}$ for the Cu-complexes and $\sim 53 \text{ cm}^{-1}$ for the Mo-

complexes), which are also considerably higher than the shift of the symmetric ν_{CO} shift of tris(1,2,4-triazolyl)borate family substituted with one to three imidazol-2-ylidene carbenes.³² Though the ν_{CO} data for the tetrakis(azolyl)borate ligands are not complete (due to the high computational costs), the tunability of the two complex groups are the highest of ~ 54 and $\sim 62 \text{ cm}^{-1}$, respectively. For borate ligands with the same number of azolyl substitutions, the pyrazolyl borates exhibit the smallest ν_{CO} and the tetrazolyl borates exhibit the largest, which implies that the metal to ligand back ($\text{M} \rightarrow \text{CO}$) π -donation is the strongest in the pyrazolyl borate complexes and the weakest in the tetrazolyl borate complexes, in line with the trend of the higher N content in the ring corresponding to its weaker electron donating capability.

Table 3. Calculated geometric parameters, NBO charges, and ν_{CO} of $[\text{Mo}(\text{O})(\text{L})_n(\text{CO})_x]^{-1}$.

ligand	$d_{\text{Mo-N}}^2$	$d_{\text{C-O}}^2$	$e(\text{B})^3$	$e(\text{Mo}(\text{CO})_x)^3$	ν_{CO}
$[\text{BH}_2(\text{pyra})_2]^-$	2.319	1.159	0.239	-0.414	1958.5
$[\text{BH}(\text{pyra})_3]^-$	2.325	1.173	0.625	-0.500	1887.3
$[\text{B}(\text{pyra})_4]^-$	2.311	1.173	1.082	-0.502	1888.9
$[\text{BH}_2(\text{inda})_2]^-$	2.316	1.157	0.232	-0.381	1966.1
$[\text{BH}(\text{inda})_3]^-$	2.304	1.171	0.617	-0.456	1900.3
$[\text{B}(\text{inda})_4]^-$	2.296	1.171	1.104	-0.463	-- ⁴
$[\text{BH}_2(\text{tria124})_2]^-$	2.320	1.157	0.228	-0.396	1966.9
$[\text{BH}(\text{tria124})_3]^-$	2.330	1.170	0.607	-0.472	1901.7
$[\text{B}(\text{tria124})_4]^-$	2.313	1.170	1.055	-0.469	1906.0
$[\text{BH}_2(\text{tria123})_2]^-$	2.317	1.157	0.227	-0.366	1970.4
$[\text{BH}(\text{tria123})_3]^-$	2.310	1.168	0.610	-0.383	1918.3
$[\text{B}(\text{tria123})_4]^-$	2.298	1.167	1.059	-0.363	1924.1
$[\text{BH}_2(\text{bentria})_2]^-$	2.300	1.157	0.220	-0.322	1979.0
$[\text{BH}(\text{bentria})_3]^-$	2.271	1.163	0.601	-0.282	1939.3
$[\text{B}(\text{bentria})_4]^-$	2.257	1.163	1.074	-0.270	-- ⁴
$[\text{BH}_2(\text{tetra})_2]^-$	2.317	1.155	0.218	-0.343	1982.1
$[\text{BH}(\text{tetra})_3]^-$	2.305	1.164	0.594	-0.335	1940.0
$[\text{B}(\text{tetra})_4]^-$	2.283	1.162	1.032	-0.302	1950.6

Notes: [1] $\nu_{\text{CO}}(\text{cm}^{-1})$ is the averaged vibration frequencies of all CO related modes in a complex. $n = 2, x = 4; n = 3 \text{ or } 4, x = 3$. [2] For bonds of the same kind, the average length (\AA) is given here, e.g. for $[\text{MoBH}_2(\text{pyra})_2(\text{CO})_4]^{-1}$, $d_{\text{C-O}}$ is the average of the four C-O bonds. [3] NBO charge. [4] The calculation was not complete due to the limited computational resources. For the full names of the azolyl groups, see Table 1.

As the coordination on boron changes, the charge on the $\text{M}(\text{CO})_x$ segment also varies. The Mo-complexes have a much bigger segment charge variation ($\sim 0.25 e$) compared with that of the Cu-complexes ($\sim 0.05 e$). As the charge on the $\text{M}(\text{CO})_x$ moiety and ν_{CO} are both determined by the borate ligand electron donating capability, we plot the $\text{M}(\text{CO})_x$ charge versus ν_{CO} for both groups of metal complexes (Figure 4). Clearly, a good linear relationship between the charge and ν_{CO} exists for the borate ligands of the same number of azolyl substitutions with each complexed metal, whereas the ν_{CO} shift is more sensitive to the segment charge change in the Cu-complexes. Bidentate borate ligands show both narrower range of the ν_{CO} shift and smaller segment charge variation, while tetrakis ones present the widest tunability in terms of both ligand tunability descriptors, which is broadened by the additive effect from all the azolyl groups.

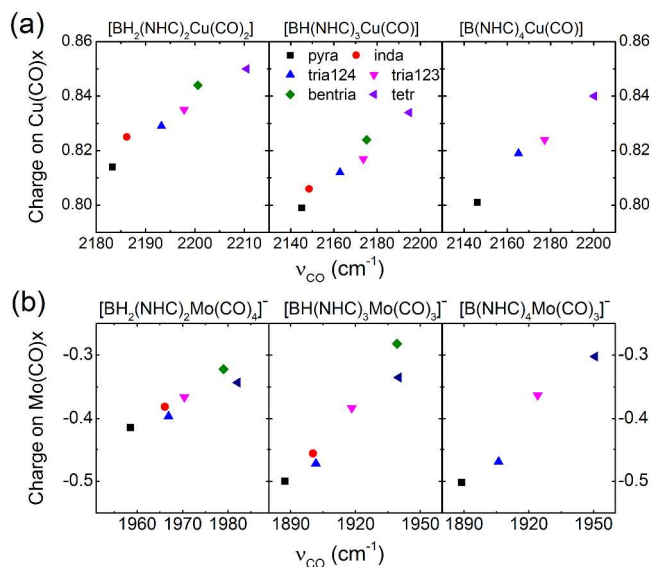


Figure 4. ν_{CO} versus the NBO charge on $\text{M}(\text{CO})_x$. (a) The neutral Cu(I)-complexes with bis- (left), tris- (middle), and tetrakis(azolyl) (right) borate ligands. (b) The anionic Mo(0)-complexes.

Conclusions

We have systematically studied a series of the poly(azolyl)borate ligands using DFT calculations. The key discoveries are summarized below.

(1) The standalone borate ligands are found to be an important and complementary case violating the "bond strength and bond length correlation", *i.e.*, with the installation of more azolyl groups on the boron center, the B-N (and B-H) bonds shrink and simultaneously become weaker, manifested in the increasingly less exothermic sequential (step-wise) bond formation energy between the azolyl group and the boron.

(2) The ligand tunability has been mapped out for the poly(azolyl)borates using the $[\text{M}(\text{L})_n(\text{CO})_x]$ model ($\text{M} = \text{Cu}(\text{I}), \text{Mo}(\text{0})$; L = the number of azolyl groups of the borate ligand; $n = 2$ to 4; x depends on M and n). Both the variation of the charge on the $\text{M}(\text{CO})_x$ moiety and the ν_{CO} shift represent the tunability of the borate ligand electron donating capability. The two descriptors (the charge $e(\text{M}(\text{CO})_x)$ and ν_{CO}) can be linearly well correlated (Figure 4). With the increase of azolyl substitution number in the borate ligands, the ν_{CO} range expands, indicating a higher tunability of the borate ligands. For the same number of azolyl substitutions, the electron donating capability of the borate ligands is inversely proportional to the N content in the azolyl ring.

(3) The ligand tunability is little influenced by metal ions and their charges.

We believe this survey on the homoleptic poly(azolyl)borate ligand family is a timely response to the recent advances in the synthetic chemistry and should be useful for the application of

the borate ligands in fine tuning the metal's electronic structures.

Acknowledgements

We are grateful for financial supports by National Science Foundation of China (Grant No. 21406175), the Scientific Research Foundation for the Returned Overseas Chinese Scholars from State Education Ministry of China (SRF for ROCS, SEM), China Postdoctoral Science Foundation (Project No.2013M542354), Shaanxi Province Postdoctoral Research Foundation, and the Fundamental Research Funds for the Central Universities.

Notes and references

^a Department of Applied chemistry, School of Science, Xi'an Jiaotong University, Xi'an, Shaanxi, 710049 China.

^b School of Materials Science and Engineering, Center for Advancing Materials Performance from the Nanoscale (CAMP-Nano), State Key Laboratory for Mechanical Behavior of Materials, Xi'an Jiaotong University, Xi'an, Shaanxi, 710049 China.

1. S. Trofimenko, *J. Am. Chem. Soc.*, 1966, 88, 1842-1844.
2. S. Trofimenko, *J. Am. Chem. Soc.*, 1967, 89, 3170-3177.
3. S. A. A. Zaidi, T. A. Khan and Z. A. Siddiqi, *Synth. React. Inorg. Met.-Org. Chem.*, 1984, 14, 717-729.
4. S. Chao and C. E. Moore, *Anal. Chim. Acta*, 1978, 100, 457-467.
5. B. Gyóri, J. Emri and L. Szilágyi, *J. Organomet. Chem.*, 1978, 152, 13-20.
6. B. Gyóri, J. Emri and P. Szarvas, *Acta. Chim. Acad. Sci. Hung.*, 1975, 86, 235-248.
7. C. Janiak, T. G. Scharmann, H. Hemling, D. Lentz and J. Pickardt, *Chem. Ber.*, 1995, 128, 235-244.
8. C. Janiak and L. Esser, *Z. Naturforsch., B: Chem. Sci.*, 1993, 48, 394-396.
9. T. A. Khan, M. ArifKhan and M. MazharulHaq, *Synth. React. Inorg. Met.-Org. Chem.*, 1996, 26, 1467-1476.
10. T. A. Khan, M. A. Khan, Z. Khan and M. M. Haq, *Synth. React. Inorg. Met.-Org. Chem.*, 2003, 33, 297.
11. F. J. Lalor, S. Miller and N. Garvey, *J. Organomet. Chem.*, 1988, 356, C57-C60.
12. G. G. Lobbia, F. Bonati and P. Ceccih, *Synth. React. Inorg. Met.-Org. Chem.*, 1991, 21, 1141-1151.
13. P. E. Szarvas, Jozsef; Gyori, Bela, *Acta. Chim. Acad. Sci. Hung.*, 1970, 64, 203-210.
14. S. A. A. Zaidi, T. A. Khan, S. R. A. Zaidi and Z. A. Siddiqi, *Polyhedron*, 1985, 4, 1163-1166.
15. K. S. Siddiqi, M. A. Neyazi and S. A. A. Zaidi, *Synth. React. Inorg. Met.-Org. Chem.*, 1981, 11, 253-265.
16. K. S. Siddiqi, M. A. Neyazi, Z. A. Siddiqi, S. J. Majid and S. A. A. Zaidi, *Indian J. Chem., Sect A*, 1982, 21A, 932-933.
17. S. Zaidi and M. Neyazi, *Transition Met. Chem.*, 1979, 4, 164-167.
18. D. Lu and C. H. Winter, *Inorg. Chem.*, 2010, 49, 5795-5797.
19. C. J. Snyder, P. D. Martin, M. J. Heeg and C. H. Winter, *Chem. Eur. J.*, 2013, 19, 3306-3310.
20. B. C. Hughes, Z. Lu and D. M. Jenkins, *Chem. Comm.*, 2014, 50, 5273-5275.

21. M. Pellei, G. G. Lobbia, G. Papini and C. Santini, *Mini-Rev. Org. Chem.*, 2010, 7, 173-203.
22. C. Santini, M. Pellei, G. G. Lobbia and G. Papini, *Mini-Rev. Org. Chem.*, 2010, 7, 84-124.
23. S. Trofimenko, *Chem. Rev.*, 1993, 93, 943-980.
24. M. Pellei and C. Santini, in *Biomimetic Based Applications*, ed. M. Cavrak, InTech, 2011, pp. 385-428.
25. M. Porchia, A. Dolmella, V. Gandin, C. Marzano, M. Pellei, V. Peruzzo, F. Refosco, C. Santini and F. Tisato, *Eur. J. Med. Chem.*, 2013, 59, 218-226.
26. M. Pellei, G. Papini, A. Trasatti, M. Giorgetti, D. Tonelli, M. Minicucci, C. Marzano, V. Gandin, G. Aquilanti, A. Dolmella and C. Santini, *Dalton Trans.*, 2011, 40, 9877-9888.
27. V. Gandin, F. Tisato, A. Dolmella, M. Pellei, C. Santini, M. Giorgetti, C. Marzano and M. Porchia, *J. Med. Chem.*, 2014, 57, 4745-4760.
28. G. L. Miessler and D. A. Tarr, *Inorganic Chemistry*, Pearson Education International, Third edn., 2004.
29. M. Casarin, L. Pandolfo and A. Vittadini, *Phys. Chem. Chem. Phys.*, 2009, 11, 94-96.
30. F. E. Jernigan, N. A. Sieracki, M. T. Taylor, A. S. Jenkins, S. E. Engel, B. W. Rowe, F. A. Jové, G. P. A. Yap, E. T. Papish and G. M. Ferrence, *Inorg. Chem.*, 2007, 46, 360-362.
31. E. T. Papish, T. M. Donahue, K. R. Wells and G. P. A. Yap, *Dalton Trans.*, 2008, 2923-2925.
32. L. Robinson, D. J. Cooke and P. I. P. Elliott, *J. Organomet. Chem.*, 2011, 696, 2580-2583.
33. Gaussian 09, Revision B.01, M. J. Frisch, G. W. Trucks, H. B. Schlegel, G. E. Scuseria, M. A. Robb, J. R. Cheeseman, G. Scalmani, V. Barone, B. Mennucci, G. A. Petersson, H. Nakatsuji, M. Caricato, X. Li, H. P. Hratchian, A. F. Izmaylov, J. Bloino, G. Zheng, J. L. Sonnenberg, M. Hada, M. Ehara, K. Toyota, R. Fukuda, J. Hasegawa, M. Ishida, T. Nakajima, Y. Honda, O. Kitao, H. Nakai, T. Vreven, J. Montgomery, J. A., J. E. Peralta, F. Ogliaro, M. Bearpark, J. J. Heyd, E. Brothers, K. N. Kudin, V. N. Staroverov, R. Kobayashi, J. Normand, K. Raghavachari, A. Rendell, J. C. Burant, S. S. Iyengar, J. Tomasi, M. Cossi, N. Rega, J. M. Millam, M. Klene, J. E. Knox, J. B. Cross, V. Bakken, C. Adamo, J. Jaramillo, R. Gomperts, R. E. Stratmann, O. Yazyev, A. J. Austin, R. Cammi, C. Pomelli, J. W. Ochterski, R. L. Martin, K. Morokuma, V. G. Zakrzewski, G. A. Voth, P. Salvador, J. J. Dannenberg, S. Dapprich, A. D. Daniels, Ö. Farkas, J. B. Foresman, J. V. Ortiz, J. Cioslowski and D. J. Fox. Gaussian, Inc., Wallingford CT, 2009.
34. A. D. Becke, *J. Chem. Phys.*, 1993, 98, 5648-5652.
35. W. J. Hehre, L. Radom, P. v. R. Schleyer and J. A. Pople, *Ab initio Molecular Orbital Theory*, Wiley, New York, 1986.
36. M. Dolg, U. Wedig, H. Stoll and H. Preuss, *J. Chem. Phys.*, 1987, 86, 866-872.
37. D. Andrae, U. Häußermann, M. Dolg, H. Stoll and H. Preuß, *Theoret. Chim. Acta*, 1990, 77, 123-141.
38. A. E. Reed, L. A. Curtiss and F. Weinhold, *Chem. Rev.*, 1988, 88, 899-926.
39. J. Catalan, R. M. Claramunt, J. Elguero, J. Laynez, M. Menendez, F. Anvia, J. H. Quian, M. Taagepera and R. W. Taft, *J. Am. Chem. Soc.*, 1988, 110, 4105-4111.
40. H. Tang and C. Wu, *ChemSusChem*, 2013, 6, 1050-1056.
41. R. B. Getman, Y. Xu and W. F. Schneider, *J. Phys. Chem. C*, 2008, 112, 9559-9572.
42. M. Kaupp, B. Metz and H. Stoll, *Angew. Chem. Int. Ed.*, 2000, 39, 4607-4609.
43. B. A. Lindquist and T. H. Dunning, *J. Phys. Chem. Lett.*, 2013, 4, 3139-3143.
44. D. V. Partyka, M. P. Washington, T. G. Gray, J. B. Updegraff III, J. F. Turner and J. D. Protasiewicz, *J. Am. Chem. Soc.*, 2009, 131, 10041-10048.
45. B. Schulze and U. S. Schubert, *Chem. Soc. Rev.*, 2014, 43, 2522-2571.
46. W. Kutzelnigg, *Angew. Chem. Int. Ed.*, 1984, 23, 272-295.